Cell Stem Cell
Article

Induction of a Hemogenic Program in Mouse Fibroblasts

Carlos-Filipe Pereira,[1,3,*] Betty Chang,[1,3,5,6] Jiajing Qiu,[1,3,5,6] Xiaohong Niu,[1,3] Dmitri Papatsenko,[1,3] Caroline E. Hendry,[1,3] Neil R. Clark,[2,3] Aya Nomura-Kitabayashi,[4] Jason C. Kovacic,[4] Avi Ma'ayan,[2,3] Christoph Schaniel,[2,3] Ihor R. Lemischka,[1,2,3,6] and Kateri Moore[1,3,6,*]
[1]Department of Developmental and Regenerative Biology
[2]Department of Pharmacology and Systems Therapeutics
[3]Black Family Stem Cell Institute
[4]Cardiovascular Research Center
[5]The Graduate School of Biomedical Sciences
Icahn School of Medicine at Mount Sinai, 1 Gustave L. Levy Place, Box 1496, New York, NY 10029, USA
[6]These authors contributed equally to this work
*Correspondence: filipe.pereira@mssm.edu (C.-F.P.), kateri.moore@mssm.edu (K.M.)
http://dx.doi.org/10.1016/j.stem.2013.05.024

SUMMARY

Definitive hematopoiesis emerges during embryogenesis via an endothelial-to-hematopoietic transition. We attempted to induce this process in mouse fibroblasts by screening a panel of factors for hemogenic activity. We identified a combination of four transcription factors, Gata2, Gfi1b, cFos, and Etv6, that efficiently induces endothelial-like precursor cells, with the subsequent appearance of hematopoietic cells. The precursor cells express a human CD34 reporter, Sca1, and Prominin1 within a global endothelial transcription program. Emergent hematopoietic cells possess nascent hematopoietic stem cell gene-expression profiles and cell-surface phenotypes. After transgene silencing and reaggregation culture, the specified cells generate hematopoietic colonies in vitro. Thus, we show that a simple combination of transcription factors is sufficient to induce a complex, dynamic, and multistep developmental program in vitro. These findings provide insights into the specification of definitive hemogenesis and a platform for future development of patient-specific stem and progenitor cells, as well as more-differentiated blood products.

INTRODUCTION

Hematopoiesis originates from multipotent hematopoietic stem cells (HSCs). These arise during development and sequentially colonize fetal liver, spleen, and finally bone marrow (BM), where they function throughout adult life. Definitive murine HSCs are first detected at embryonic day 10.5 (E10.5) in clusters associated with the ventral floor of the dorsal aorta in the aorta-gonad-mesonephros (AGM) region and after E11.5 in the fetal liver, yolk sac, and placenta (reviewed by Medvinsky et al., 2011). It is thought that HSCs emerge from a small population of "hemogenic" endothelial cells (Bertrand et al., 2010; Boisset et al., 2010; Eilken et al., 2009; Kissa and Herbomel, 2010; Lancrin et al., 2009).

Several transcription factors (TFs) have been implicated in endothelial-to-hematopoietic transition and HSC specification, including Runx1 (North et al., 1999), Scl (Porcher et al., 1996), Gata2 (Tsai et al., 1994), Gfi1/Gfi1b (Lancrin et al., 2012), and Notch1 (Kumano et al., 2003). Mutant $Scl^{-/-}$ or $Runx1^{-/-}$ embryos have no AGM clusters or hematopoietic stem and progenitor cells (HSPCs) (North et al., 1999; Porcher et al., 1996). Specific deletion of Runx1 in the endothelium and in emergent HSCs inhibits cluster formation and hematopoietic specification (Li et al., 2006). Recently, it has been suggested that Sca1, encoded by the *Ly6a* gene, marks hemogenic endothelial cells. Indeed, *Ly6a*-driven expression of Cbfβ, a Runx1 cofactor, rescues production of HSCs (Chen et al., 2011). Mutant $Notch1^{-/-}$ embryos lack definitive hematopoiesis although they develop normal numbers of yolk-sac progenitors (Kumano et al., 2003). Several TFs have been implicated in HSC self-renewal. Specifically, deletions of Etv6 (Hock et al., 2004b), PU.1 (Burda et al., 2010), Gfi1 (Hock et al., 2004a), or Gata2 (Rodrigues et al., 2005) result in adult HSC defects, whereas loss of Sox17 causes defects in fetal-liver HSCs (Kim et al., 2007). Gain-of-function studies have identified factors such as HoxB4, HoxA9, PU.1, Erdr1, and cFos that expand HSC activity (Deneault et al., 2009). Despite the accumulating molecular data, in vitro efforts to produce transplantable HSCs from embryonic stem cells (ESCs) have been largely unsuccessful. Dissecting the hemogenic process may provide key insights for the in vitro generation of definitive HSCs.

Studies by Yamanaka and colleagues demonstrated that Oct4, Sox2, Klf4, and cMyc can reprogram fibroblasts into induced pluripotent stem cells (iPSCs) (Takahashi and Yamanaka, 2006). Defined TFs can also interconvert differentiated cell types (reviewed by Pereira et al., 2012). Recently, Sox2 alone or in combination with other TFs has been used to convert fibroblasts into neural stem cells (Lujan et al., 2012; Ring et al., 2012). Collectively, these studies led us to ask whether a minimal number of TFs can specify definitive hematopoiesis and HSCs.

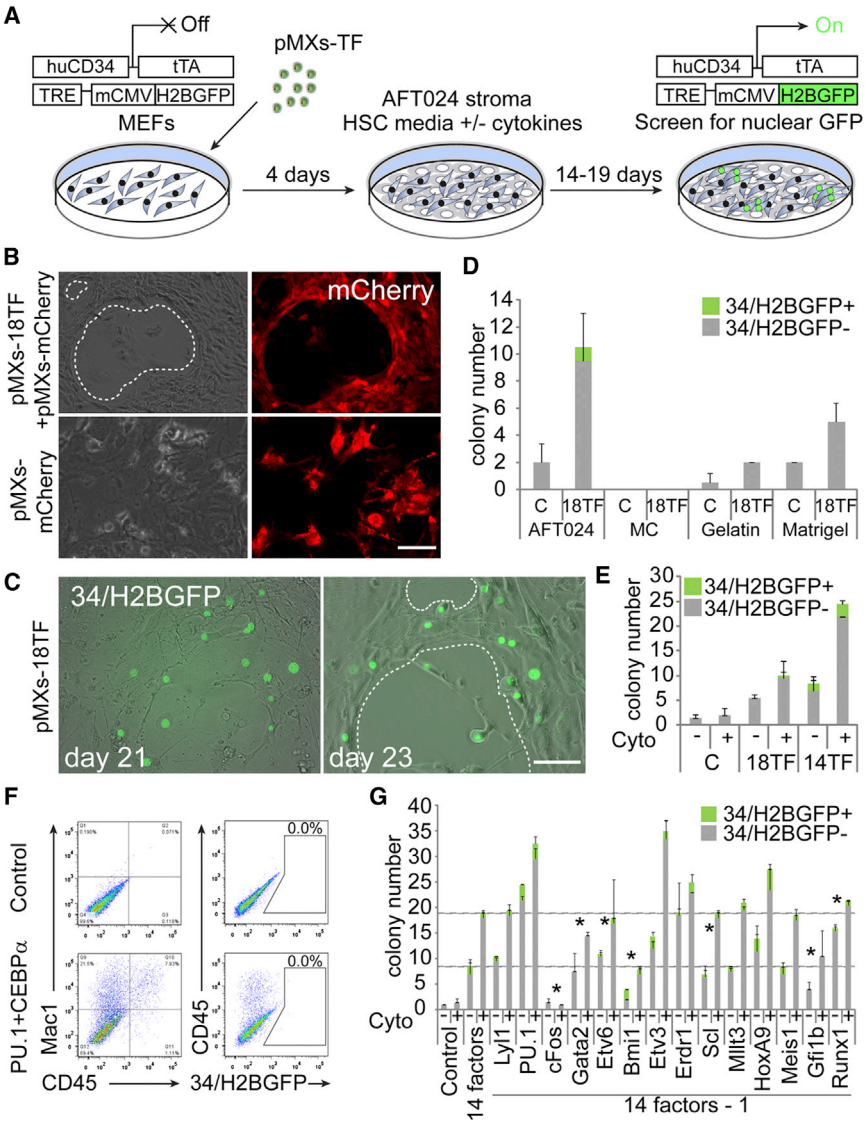

Figure 1. Screening for Hematopoietic Fate-Inducing Factors

(A) Strategy for testing hematopoiesis-inducing factors. Mouse MEFs were isolated from 34/H2BGFP double-transgenic mice and transduced with pools of candidate TFs (pMXs-TFs). Four days after transduction, MEFs were replated onto AFT024 stroma with or without cytokines (SCF, Flt3l, IL-3, and IL-6), cocultured for 14–19 days, and screened for GFP via immunofluorescence and flow cytometry.

(B) MEFs transduced with pMXs-mCherry or the 18-TF cocktail plus mCherry were analyzed at day 21. The emergence of colonies was observed only in the 18-TF pool + mCherry (upper panels) and not in the mCherry control (lower panels). mCherry (red) shows the MEF origin of colonies and bright field shows morphologies.

(C) A single colony was assayed for 34/H2BGFP activation (green) 21 and 23 days after transduction with 18 TFs. Dashed lines highlight morphological changes. Scale bars represent 100 μm.

(D) MEFs were transduced with 18 TFs or empty vector control (C) and transferred to AFT024, methylcellulose-containing media (MC), gelatin, or Matrigel-coated dishes with cytokines. GFP^+ and GFP^- colonies were counted via immunofluoresence and bright-field microscopy at 21 days.

(E) MEFs were transduced with retroviral pools expressing 18 TFs, 14 TFs, or empty vector control (C) and cultured with (+) and without (−) cytokines (Cyto) on AFT024 stroma.

(F) 34/H2BGFP MEFs were transduced with PU.1 + CEBPα. FACS plots show the expression of CD45, Mac1, and no activation of 34/H2BGFP at day 8.

(G) GFP^+ and GFP^- colonies after removal of individual factors from the 14-TF pool. Factors whose removal decreased colony numbers were selected (asterisks). Colony numbers are per 10,000 infected MEFs (mean ± SEM).

See also Figure S1.

We show that the four TFs, Gata2, Gfi1b, cFos, and Etv6, convert fibroblasts into endothelial-like cells that subsequently generate HSPC-like cells. These cells adopt emergent HSC-like gene-expression profiles and cell-surface phenotypes. This is the first demonstration that a complex developmental process can be "set in motion" in vitro by a defined combination of TFs.

RESULTS

A Screen for Hematopoiesis-Inducing Transcription Factors

Two approaches were used to identify candidate TFs: (1) literature mining and (2) global profiling for defining genes with high expression levels in HSCs relative to mature blood cells and other tissues. Profiling studies utilized BM HSCs isolated from a double-transgenic mouse, huCD34tTA × TetO-H2BGFP (hereafter called 34/H2BGFP). H2BGFP is specifically expressed in immature HSPC compartments, and cells with long-term-repopulating (LT)-HSC cell-surface phenotypes have the highest GFP levels (Schaniel and Moore, 2009). Synthesis of H2BGFP is turned off by doxycycline (Dox) administration, and the label is progressively diluted via cell division. Dormant, nondividing HSCs retain high levels of GFP and have very robust in vivo repopulation activity, whereas active dividing cells lose activity (J.Q. and K.M., unpublished data). HSCs with progressively decreasing levels of GFP were profiled for identification of the TFs present in the brightest population. Using this method together with data mining, a total of 18 TFs were identified (Figures S1A and S1B and Table S1 available online).

All 18 TFs were individually inserted into the pMXs retroviral vector. Target mouse embryonic fibroblasts (MEFs) were obtained from 34/H2BGFP embryos. The reporter should be reactivated when a hematopoietic or endothelial progenitor fate is acquired (Radomska et al., 2002) (Figure 1A). To eliminate contamination with hematopoietic and very rare GFP^+ cells, we removed residual $CD45^+$ and GFP^+ cells via cell sorting prior to

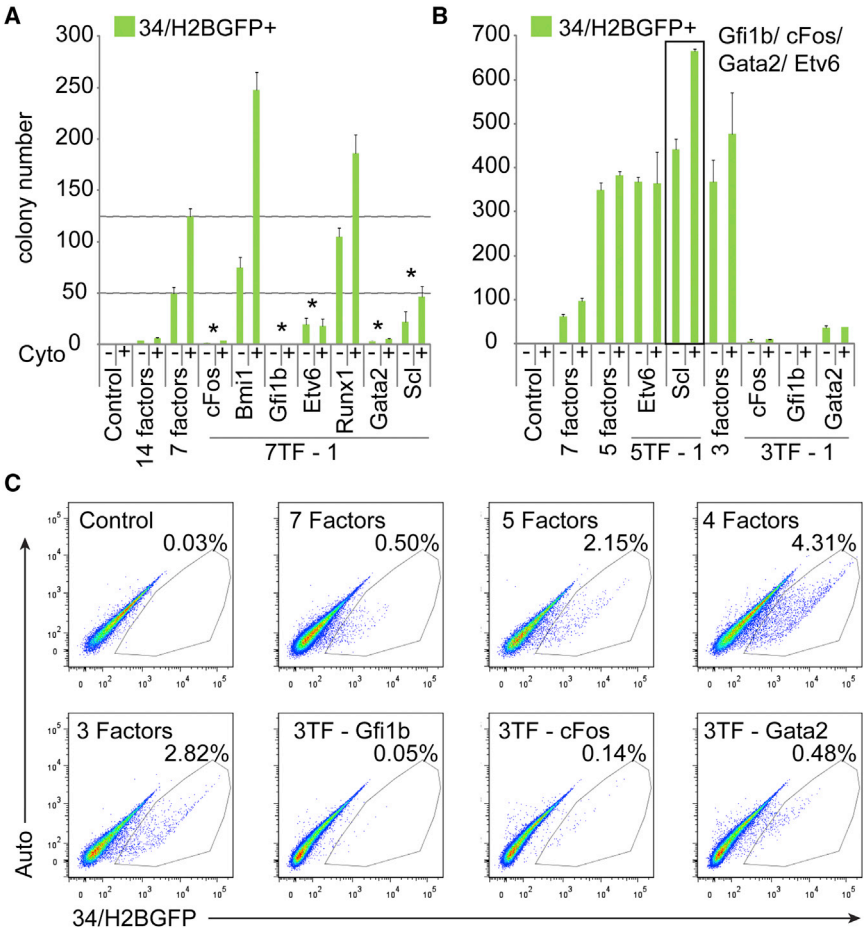

Figure 2. Combination of Gata2, Gfi1b, cFos, and Etv6 Induces Efficient Activation of 34/H2BGFP

(A and B) GFP$^+$ colony numbers were counted after removal of individual TFs from the pool of seven TFs (Gfi1b/cFos/Gata2/Etv6/Scl/Bmi1/Runx1) (A), five TFs (Gfi1b/cFos/Gata2/Etv6/Scl), and three TFs (Gfi1b/cFos/Gata2) (B). Fluorescent colonies were counted 22 days after transduction with (+) or without (–) cytokines. TFs whose removal decreased the colony number were selected (asterisks). Four TFs (Gfi1b/cFos/Gata2/Etv6) yielded the optimal efficiency of activation (4%–7%). Colony numbers per 10,000 infected MEFs are shown (mean ± SEM).

(C) MEFs were analyzed via flow cytometry 22 days after transduction with pools of seven, five, four, three (Gfi1b/cFos/Gata2), or two TFs (3F – the indicated TF). The percentages of GFP$^+$ cells are shown. Auto, autofluorescence.

See also Figure S2.

transduction. MEFs were transduced with the 18-TF cocktail and plated 4 days later on AFT024 HSC-supporting stromal cells (Moore et al., 1997). After 21 days, we observed the emergence of colonies organized into circular structures (Figure 1B and Figure S1C). These structures continued over time, and rare colonies expressed nuclear GFP, reflecting 34/H2BGFP activation (Figures 1C and S1D). Colonies or GFP$^+$ cells were never observed with control vectors. We next investigated the reprogramming conditions using a variety of substrates, including AFT024, methylcellulose, gelatin, and Matrigel. AFT024 cocultures yielded the highest colony numbers and were the only condition supporting reporter activation (Figure 1D). To identify the critical TFs, we sequentially removed factors from the starting cocktail. Because of their broader expression in dormant and active HSCs as well as in other tissues, Trib3, Bex2, Tcf3, and Hhex were initially removed, yielding a cocktail of 14 TFs (Figures S1A and S1B). MEFs transduced with the 14 TFs were cocultured with AFT024 with or without cytokines. GFP$^+$ and GFP$^-$ colonies were quantified after 18 days. We observed increases in total and GFP$^+$ colony numbers, and the latter appeared without cytokines (Figure 1E). As an additional control for 34/H2BGFP reporter specificity, CEBPα and PU.1 were used to convert MEFs into macrophage-like cells (Feng et al., 2008), and as expected, no reporter activation was observed (Figure 1F).

Gata2, Gfi1b, cFos, and Etv6 Are Sufficient for Efficient 34/H2BGFP Activation

We next deleted individual TFs from the pool of 14 (Figure 1G). Removal of PU.1, Etv3, HoxA9, or Erdr1 yielded increased total and GFP$^+$ colony numbers. Deletion of Lyl1, Scl, Mllt3, and Meis1 did not significantly alter colony numbers. Removal of Gata2, Gfi1b, or cFos reduced colony numbers and abolished GFP$^+$ colonies, showing that these are essential. Removal of Bmi1 decreased GFP$^-$ colony numbers. We selected seven TFs (Gata2, Gfi1b, cFos, Etv6, Scl, Bmi1, and Runx1) for subsequent studies. Scl and Lyl1 are largely redundant (Souroullas et al., 2009), and this is probably also the case for Etv6, Etv3, and PU.1. We retained Runx1 because of its requirement in the endothelial-to-hematopoietic transition (Li et al., 2006). Transduction with seven TFs produced a 14-fold increase in GFP$^+$ colonies relative to the pool of 14 (3.5 to 50) (Figure 2A). Addition of cytokines resulted in a 1.5- to 3-fold increase in total colony numbers and in larger GFP$^+$ colonies (Figures 2A and S3A). Two additional rounds of factor removal showed that four TFs (Gata2, Gfi1b, cFos, and Etv6) were sufficient for 34/H2BGFP activation (Figure 2B). Activation efficiency after 22 days was also dramatically increased (4%–7%) (Figures 2B and 2C). Removal of Etv6 slightly reduced the percentage of GFP$^+$ cells (4.3% to 2.8%), whereas exclusion of each of the remaining three (Gata2, Gfi1b, and cFos) had a dramatic negative impact on GFP$^+$ cells. We next analyzed the in vivo expression patterns of the four TFs. *Gata2*, *Gfi1b*, and *Etv6* messenger RNAs (mRNAs) are enriched in both phenotypically defined and dormant HSCs (Figure S2). Vector integration was also confirmed in GFP$^+$ cells generated with 11 and 4 TFs (Figure S2D).

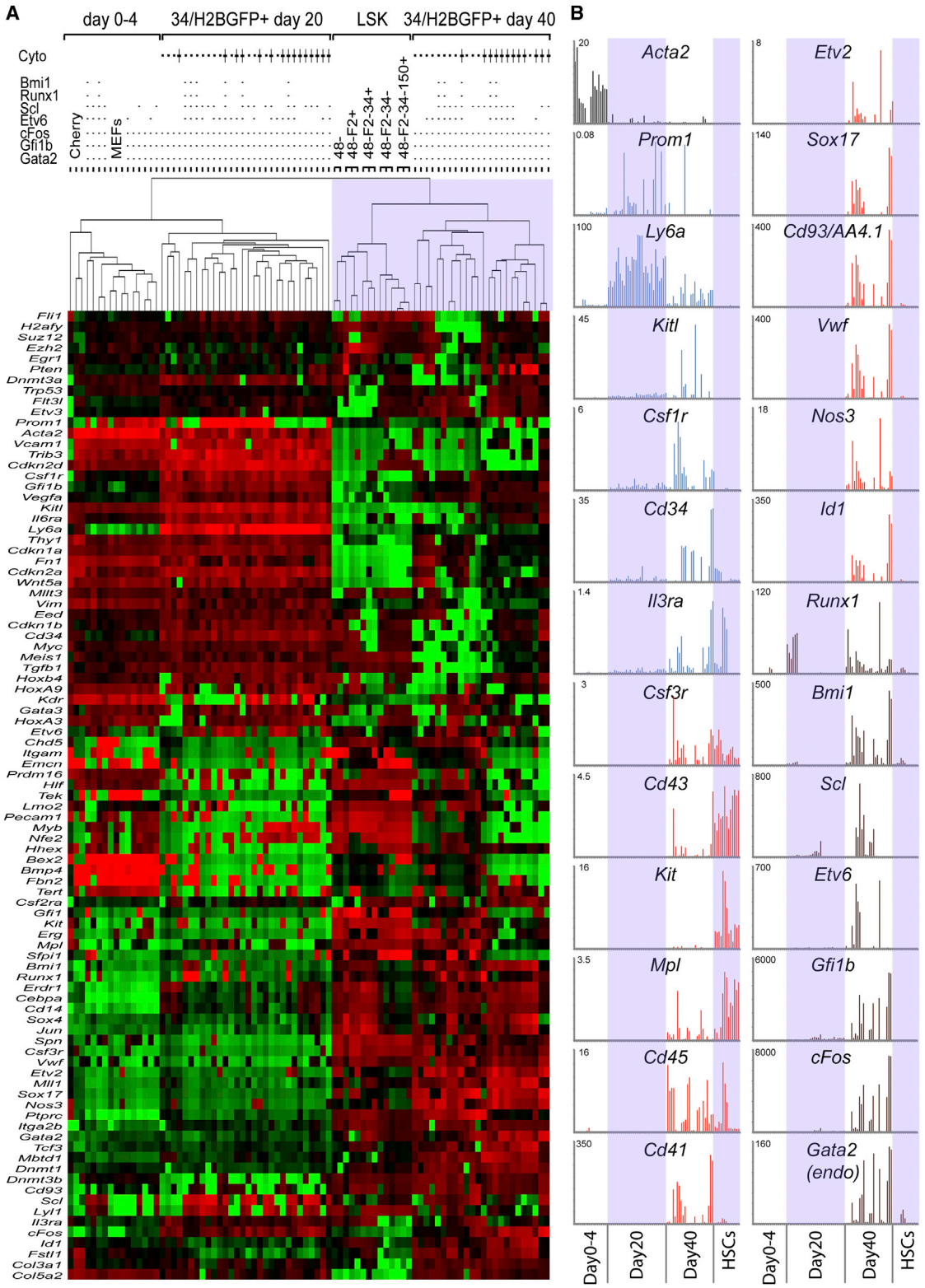

Figure 3. Induced 34/H2BGFP$^+$ Cells Express Endothelial and Hematopoietic Markers Similarly to HSCs

(A) 34/H2BGFP MEFs were transduced with pools of seven, five, four, or three TFs (as indicated by dots in the upper panel) and cocultured with AFT024 stroma with (+) or without (–) cytokines. At day 0 (MEFs), day 4, day 20, and day 40 after transduction, groups of 100 GFP$^+$ cells were sorted and assayed for expression. MEFs transduced with pMXs-mCherry were included as controls. Levels of mRNA expression were compared to purified HSC populations isolated from the BM of 34/H2BGFP mice (from left to right: LSKCD48$^-$, LSKCD48$^-$Flk2$^+$, LSKCD48$^-$Flk2$^-$CD34$^+$, LSKCD48$^-$Flk2$^-$CD34$^-$, LSKCD48$^-$Flk2$^-$CD34$^-$CD150$^+$). Red

(legend continued on next page)

Cells with Activated 34/H2BGFP Express Endothelial and Hematopoietic Genes

To characterize gene expression in GFP$^+$ cells, we used the Fluidigm BioMark system. Reporter MEFs were transduced with pools of seven, five, four, or three TFs and cultured with AFT024 for 20 and 40 days with and without cytokines (Figure 3A, upper panel). Nontransduced and mCherry-transduced MEFs as well as GFP$^+$ cells from TF-transduced samples were sorted into 96-well plates (100 cells per sample per well in duplicate or triplicate). Gene-expression patterns were compared to BM HSPC populations isolated from adult 34/H2BGFP mice. Dramatic gene-expression changes in transduced cells (relative to MEFs) were observed at days 20 and 40. GFP$^+$ cells show time-dependent transcriptional changes, highlighting the dynamic nature of the induction process. Remarkably, unsupervised hierarchical clustering placed day 40 GFP$^+$ cells generated without cytokines closest to bona fide adult HSCs (Figure 3A). We observed decreased expression of fibroblast-specific genes such as *Vim*, *Acta2*, *Fn1*, and *Fbn2* between days 0 and 20 (Figures 3A and 3B). At day 20 we detected high levels of *Prom1* (Prominin1) and *Ly6a*, as well as activation of *KitL*, *Csf1r*, *Cd34*, and *Il3ra* (Figure 3B). Expression profiles do not show major differences in GFP$^+$ cells generated with different TF pools (as long as Gata2, Gfi1b, and cFos are present). Thus, the additional factors affect the efficiency, but not the global reprogramming of gene expression. At day 40 we detected coexpression of hematopoietic (*Csf3r*, *Il3ra*, *Cd43*, *Kit*, *Mpl*, *Cd45*, and *Cd41*) and endothelial and/or endothelial progenitor markers (*Vwf*, *Nos3*, and *Id1*). Interestingly, at day 40 we detected markers of emergent and fetal HSCs (*Cd93/AA4.1*, *Cd41*, and *Sox17*) and hemogenic endothelium (*Etv2* and *Runx1*) (Figure 3B). Using specific primers we also demonstrated expression of endogenous *Gata2* (Figure 3B).

Sequential Induction of Precursor and Hemogenic Colonies with Gata2, Gfi1b, cFos, and Etv6

To further characterize emerging cells, we examined the expression of Sca1 and Prom1. After 22 days, 50%–60% of the GFP$^+$ cells were Sca1$^+$ (data not shown), and 36% were Prom1$^+$ (Figure 4A). Prom1$^+$ cells also expressed high levels of Sca1 (89%), confirming our mRNA analyses in day 20 GFP$^+$ cells (Figure 3B). The four-TF cocktail (Gata2, Gfi1b, cFos, and Etv6) induced higher percentages of GFP$^+$Prom1$^+$ cells in comparison to seven and five factors and other combinations of four factors (Figure 4B).

At 35 days, we observed emergence of colonies containing clusters of nonadherent GFP$^+$ cells (Figure 4C). Remarkably, we identified clusters that express the endothelial markers Tie2, CD31, VE-Cadherin, and the panhematopoietic marker CD45 (Figure 4C). We next sought to determine optimal conditions for generating hematopoietic cell clusters. With four TFs, AFT024 was no longer necessary for generating day 20 GFP$^+$ or day 35 nonadherent hematopoietic cell clusters (Figures S3A, S3B, and S3C). In addition, inclusion of cytokines decreased the numbers of nonadherent cells. Cultures on gelatin without cytokines yielded 9% CD45$^+$ cells at day 35 (Figure S3D). We tested the effects of individual cytokines and found that interleukin-6 (IL-6) is inhibitory (2% CD45$^+$), whereas IL-3 has a positive effect (27% CD45$^+$) (Figures S3D and S3E). The latter may be due to the expansion of CD45$^+$ cells or maturation from precursor endothelial-like cells as previously reported in mouse AGM (Taoudi et al., 2008). Kinetic analyses of endothelial and hematopoietic markers showed that Tie2 expression is transient whereas CD45 expression increases steadily over time (Figure 4D). This is consistent with the role of Gfi1b in loss of endothelial identity (Lancrin et al., 2012).

Between days 30 and 40, we identified several cellular components in GFP$^+$ cultures (Figure 4E) associated with emergence of CD45$^+$ cells: (1) small nonadherent or semiadherent GFP$^+$CD45$^+$ cells with compact nuclei, (2) large adherent GFP$^+$CD45$^-$ cells often found in the margins of circular structures, and (3) very large adherent GFP$^+$CD45$^-$ cells that contain one or more nuclei. CD45$^+$ cells are often seen in association with GFP$^+$CD45$^-$ cells, particularly when semiadherent (Figure 4E, right panel). We monitored emergence of CD45$^+$ cells by using time-lapse imaging for morphology,reporter activation, and live staining for CD45 (Movie S1). We found that small GFP$^+$CD45$^-$ cells are associated with large adherent cells. Acquisition of CD45 is often accompanied by dissociation of nonadherent cells from large cells that then die (Movie S2).

In order to determine whether we could isolate the precursor for the emergent hematopoietic cells, we sorted the GFP$^+$Sca1$^+$ Prom1$^+$ population and cultured it on gelatin (Figure 4F, left panels). After 6 days, we observed a higher percentage of CD45$^+$ cells in cultures initiated with the sorted cells (53%) than in those initiated with the unsorted population (9%) (Figure 4F, right panel). CD45$^+$GFP$^+$ cells emerge in association with large, flat CD45$^-$GFP$^+$ cells (Figure 4F, middle panels), which are also Mac1 negative (data not shown). These data suggest that GFP$^+$Sca1$^+$Prom1$^+$ cells are hemogenic precursors.

Precursor GFP$^+$ Cells Display an Endothelial-like Gene-Expression Signature

To better define the precursor and emergent hematopoietic cells, we performed mRNA sequencing (mRNA-seq) on populations generated after transduction with Gata2, Gfi1b, cFos, and Etv6. Two biological replicates were sorted from nontransduced MEFs, day 20 GFP$^+$Sca1$^+$Prom1$^+$ cells, and the cKit$^+$ and cKit$^-$ subsets within the day 35 GFP$^+$CD45$^+$ population (Figure S4A). Replicates correlate with each other, in contrast to comparisons between different samples (Figures S4B and S4C). We used nonnegative matrix factorization coupled with consensus clustering to analyze sample diversity and showed that MEFs are followed by day 20 cells and day 35 cKit$^+$ and cKit$^-$ cells (Figure 5B,

indicates increased expression and green indicates decreased expression over the mean. Shading highlights the similarity between day 40 samples and BM HSCs. Data were normalized to *Hprt* expression, analyzed by Cluster 3.0, and displayed by TreeView.

(B) Relative mRNA expression levels of fibroblast-associated genes (*Acta2*; highlighted in black) and markers with expression initiated at day 20 (*Prom1*, *Ly6a*, *Kitl*, *Csf1r*, *Cd34*, and *Il3ra*; highlighted in blue). Expression of hematopoietic (*Csf3r*, *Cd43*, *Kit*, *Mpl*, *Cd45*, and *Cd41*), endothelial (*Vwf*, *Id1*, and *Nos3*), and emerging HSC markers (*Sox17* and *Cd93/AA4.1*) (red). Expression of *Runx1*, *Bmi1*, *Scl*, *Etv6*, *Gfi1b*, and *cFos* total mRNAs (transgene + endogenous) and endogenous *Gata2* (endo; brown). Transductions from seven to three TFs are ordered from left to right. Expression levels are relative to *Hprt*.

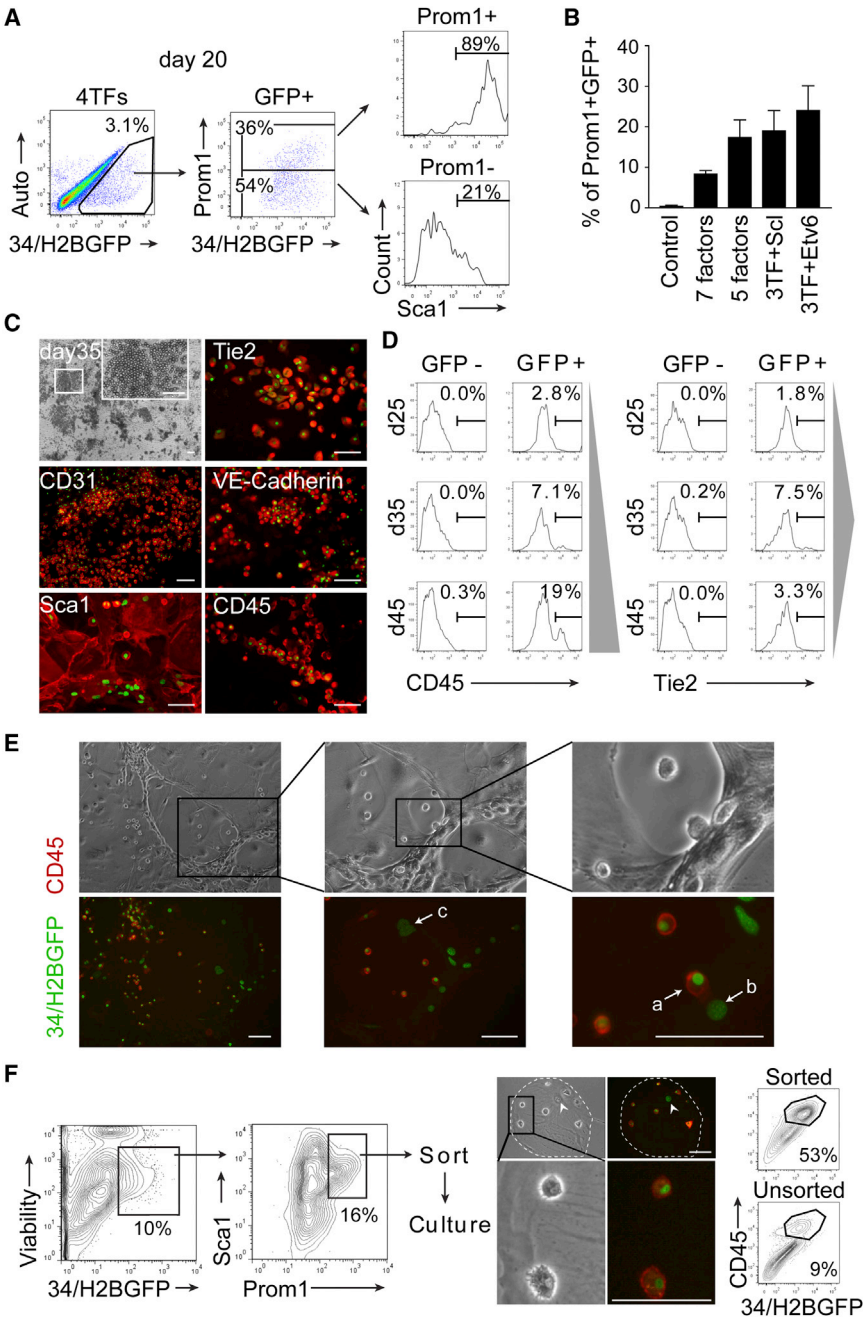

Figure 4. Induced Hemogenic Colonies Emerging from a Precursor Cell Type

(A) MEFs were transduced with four TFs (Gata2, Gfi1b, cFos, and Etv6) and cultured on AFT024 stroma with cytokines. At day 20, GFP$^+$ cells were analyzed for expression of Prom1 and Sca1.

(B) Quantification of the Prom1$^+$GFP$^+$ cell percentage after transduction with seven, five, or four TFs. The highest percentage was achieved by transduction with Gfi1b, cFos, Gata2, and Etv6 (3F + Etv6, mean ± SEM).

(C) MEFs were transduced with seven TFs, cultured on AFT024 stroma without cytokines, and analyzed at day 35 via immunofluorescence. The emergence of nonadherent cells is shown. The insert shows a higher magnification to highlight round, nonadherent cells. Shown in red is live staining for Tie2, CD31, VE-cadherin, Sca1, and CD45 as indicated, and GFP expression is shown in green.

(D) MEFs were transduced with four TFs, cultured on gelatin, and analyzed sequentially at days 25, 35, and 45. The percentages of CD45$^+$ and Tie2$^+$ cells are shown in gated GFP$^+$ and GFP$^-$ populations. A representative experiment of three is shown.

(E) MEFs were transduced with four TFs, plated on gelatin without cytokines, and analyzed at 40 days with immunofluorescence. GFP (green), CD45 staining (red), and bright field show the morphology. The following cellular components are highlighted with arrows: (a) small nonadherent or semiadherent GFP$^+$CD45$^+$ cells, (b) larger adherent GFP$^+$CD45$^-$ cells, and (c) very large adherent GFP$^+$CD45$^-$ cells.

(F) GFP$^+$Sca1$^+$Prom1$^+$ cells were isolated at day 20 after transduction with four TFs and replated on gelatin (left). After 6 days, cultured cells were analyzed via immunofluorescence and flow cytometry (right panels). CD45$^+$ (red) and GFP$^+$ (green) cells emerge in the cultures. Cell boundaries (dashed line) and nuclei (arrowhead) of bigger CD45$^-$ cells are highlighted. The insert shows a higher magnification to highlight GFP$^+$ CD45$^+$ cells. Scale bars represent 100 μm. Flow plots (far-right panels) show the enrichment of CD45$^+$ emerging in cultures of sorted versus unsorted populations. See also Figure S3.

upper panel). This is consistent with morphological changes (Figure 5A) and the Fluidigm data (Figure 3). Metagene analysis showed sets of genes expressed in MEFs and silenced in all other samples (Figure 5B, lower panel), genes expressed transiently at day 20, and genes that are expressed in CD45$^+$ cKit$^+$ cells and either silenced or also expressed in CD45$^+$cKit$^-$ cells. Metagenes identified in CD45$^+$cKit$^+$ and CD45$^+$cKit$^-$ cells show higher overlap than those in MEFs and at day 20 (Figure 5B, lower panel). Principal component analysis (PCA) placed MEFs and day 20 and day 35 CD45$^+$ cells very distant from each other, demonstrating the striking phenotypic transition from MEFs to day 20 precursors and subsequently to CD45$^+$ cells. CD45$^+$cKit$^+$ and CD45$^+$cKit$^-$ are closely related but clearly distinguishable by PCA (Figure 5C).

Alignment of reads at individual gene loci and quantification by fragments per kilobase of exon per million fragments mapped (FPKM) values confirm silencing of MEF genes *Acta2*, *Fbn1*, *Fbn2*, *Fn1*, and *Col5a2* (Figures 5D and 5E). *Ly6a* was upregulated 6-fold at day 20, whereas *Ly6e* was upregulated 2.8-fold in CD45$^+$cKit$^+$ cells. Both *Ly6a* and *Ly6e* genes encode the Sca1 antigen. *CD45* was only detected in day 35 CD45$^+$ cells (Figure 5D). At day 20, proposed markers of AGM HSC precursors including podocalyxin-like protein 1 (*Pclp-1*) (Hara et al., 1999) and the angiotensin-converting enzyme (*Ace*) (Sinka et al., 2012) were detected. *Pclp-1*, *Podxl2*, and *Ace* are upregulated 120-, 5-, and 9-fold, respectively (Figure 5E).

Proangiogenic factors such as *Hand2*, *Kdr*, *Tgfb2*, *Itga6*, *Notch4*, *KitL*, and *Proliferin 2/3 (Plf-2/3)* were also detected at day 20 (Figure 5E). Indeed, pathway analysis using the PANTHER classification system showed enrichment of pathways related to endothelial biology. These include angiogenesis (p value = 2.5×10^{-04}), Vegf (p value = 5.0×10^{-04}), Tgfβ (p value = 1.0×10^{-03}), and Integrin signaling (p value = 1.8×10^{-04}) (Figure S5B), as well as heterotrimeric G protein signaling, endothelin signaling, and cytokine-mediated inflammation, a process that may be involved in hemogenesis (Figure S5). Gene ontology (GO) analysis showed that the extracellular region or matrix, the actin cytoskeleton, and cell junctions were enriched cellular component categories. Top molecular function and biological process GO categories were protein and receptor binding, receptor activity, cell communication, and signal transduction (Figure S5). Together, these analyses demonstrate that in GFP$^+$ Sca1$^+$Prom1$^+$ precursors, an endothelial-like gene-expression program precedes the activation of a hematopoietic program in emerging CD45$^+$ cells. Some genes, such as *Itga6* (encoding CD49f), are expressed in precursor cells, and their expression is maintained in emergent hematopoietic cells. Analysis of CD49f protein confirmed expression in the emergent hematopoietic and endothelial-like cells (Figures 5F and 5G). Analysis of genes upregulated in day 35 CD45$^+$cKit$^+$ cells using the Mouse Genome Informatics (MGI) mouse mutant phenotype database showed that genetic perturbations cause largely hematopoietic phenotypes (Figure 5H, right panel). In contrast, genes upregulated at day 20 impact blood vessel and embryo development, as well as other processes (Figure 5H, left panel). MicroRNA (miRNA) target prediction focused on genes activated between day 20 and day 35 CD45$^+$cKit$^+$ cells showed highest enrichment of miR-125 targets (Figure 5I, right panel; p value = 8.48×10^{-04}). MiR-125 is highly expressed in HSCs and was shown to expand their numbers in vivo (Guo et al., 2010). Targets of several other miRNAs implicated in HSPCs (miR-29, miR-142, miR-19, miR-130, and miR-520) were also identified. In contrast, at day 20 a different set of miRNA targets were identified, including those for the vascular-endothelium-specific miR-15 (Figure 5I, left panel; p value = 8.56×10^{-03}) (Yin et al., 2012) and others related to endothelial cell biology (miR-99, miR-200, miR-519 and miR-135).

Emergent Hematopoietic Cells Express Markers of Definitive Hematopoiesis

We used gene set enrichment analysis (GSEA) to compare the transition of day 20 precursors to day 35 CD45$^+$cKit$^+$ cells with published gene sets (Figure 6A). This showed significant enrichment of GSEA database HSC gene sets in the CD45$^+$cKit$^+$ samples (24 out of 35 HSC gene sets; Fisher's exact test, p value = 6.6×10^{-04}; false discovery rate [FDR] < 0.25). Indeed, the most enriched gene set among the 1,888 in the database was an HSC gene set (Table S6). Next, we determined whether immune signaling pathways were enriched in the CD45$^+$cKit$^+$ population. Curated immune signaling pathways (32 out of 32) were enriched in CD45$^+$cKit$^+$ cells including the Kit receptor, IL-3, and B and T cell receptor, in agreement with hematopoietic specification. We next used GSEA to compare CD45$^+$cKit$^+$ to CD45$^+$ cKit$^-$ cells (Figure 6B). Consistent with PCA (Figure 5C), fewer gene sets were enriched than in comparison to day 20 cells. Four HSC gene sets were enriched, including three from LT-HSCs. More-significant enrichment of LT-HSC gene sets was found in the CD45$^+$cKit$^+$ sample (3 out of 3 LT-HSCs gene sets; Fisher's exact test, p value = 5.1×10^{-05}, FDR < 0.35). The enriched signaling pathways include Hedgehog, Wnt, α6β4 Integrin, and OSM, consistent with their roles in hemogenesis. To address whether the induced hematopoietic cells were closest to "specifying" versus "definitive" HSCs, we compared our data to the recently published data sets from BM, fetal-liver, placenta, AGM, and yolk-sac HSCs (McKinney-Freeman et al., 2012). Remarkably, the specified CD45$^+$cKit$^+$ and CD45$^+$ cKit$^-$ cells show a robust clustering, with nascent HSCs prospectively isolated from the AGM, placenta, and early fetal liver (Figure 6C).

Global analysis also revealed activation of HSC transcriptional regulators including *Scl*, *Fli1*, *Hhex*, *Smad6*, *Lyl1*, *Lmo2*, *Runx1*, *Sox17*, *Msi2*, and *Gfi1*. Master regulators of the lymphoid (*Ikzf1*), myeloid (*PU.1*) and erythroid (*Eto2* and *Fog1*) lineages were also expressed in CD45$^+$cKit$^+$ and CD45$^+$cKit$^-$ cells (Figure 6D). We next analyzed genes in the Notch signaling pathway because of its role in the onset of definitive, but not primitive, hematopoiesis (Kumano et al., 2003). *Notch1* and *Notch2* were both upregulated in CD45$^+$ cells, and the former was more highly expressed in CD45$^+$cKit$^+$ cells and the latter in CD45$^+$cKit$^-$ cells (Figures 6D and 6E). Another marker of definitive hematopoiesis is the Cxcr4 pathway (Moepps et al., 2000). *Cxcr4* is expressed in CD45$^+$ cells along with downstream genes (Figure 6F). HSCs and immature progenitors silence Moloney-based retrovirus (Klug et al., 2000). We analyzed pMXs proviral expression by aligning mRNA-seq reads against the pMXs sequence (Figure 6G). Retroviral sequences were detected at day 20, consistent with transgene expression (Figure 3B). In CD45$^+$ cells, pMXs sequences were detected in the CD45$^+$cKit$^-$ compartment with a 10-fold reduction in CD45$^+$cKit$^+$ cells, consistent with silencing in HSCs and immature progenitors (Figure 6G). Collectively, these results highlight the definitive hematopoietic nature of cells specified by the four TFs.

Specified Cells Contain Cells with an LT-HSC Cell-Surface Phenotype and Generate Colonies In Vitro after Reaggregation Culture

We then asked whether global gene expression is reflected in a LT-HSC cell-surface phenotype. Among Sca1$^+$ cells, 17% were also CD45$^+$ and GFP$^+$ (Figure 7A, left panels). This compartment contained cells with a CD48$^-$CD150$^+$cKit$^+$ LT-HSC phenotype, whereas the CD45$^-$ compartment did not (Figure 7A, right panels). To address the clonogenic function of specified hematopoietic cells, we transferred Gata2, cFos, Gfi1b, and Etv6 into Dox-inducible lentiviral vectors (Tet-On system, strategy outlined in Figure S6) to avoid the complications of continued overexpression or re-expression of TFs. When cultured with Dox, the transgenes are expressed, and upon Dox withdrawal, transgene expression is significantly reduced (days 1–3), becoming undetectable after 6 days (Figure S6A). Expression of Gata2, cFos, Gfi1b, and Etv6 driven by these vectors in MEFs from wild-type C57Bl6 mice first induces precursor cells and, upon continued culture with Dox, the emergence of nonadherent CD45$^+$ hematopoietic cells (Figure S6B). Isolation of emergent CD45$^+$ cells by fluorescence-activated cell sorting

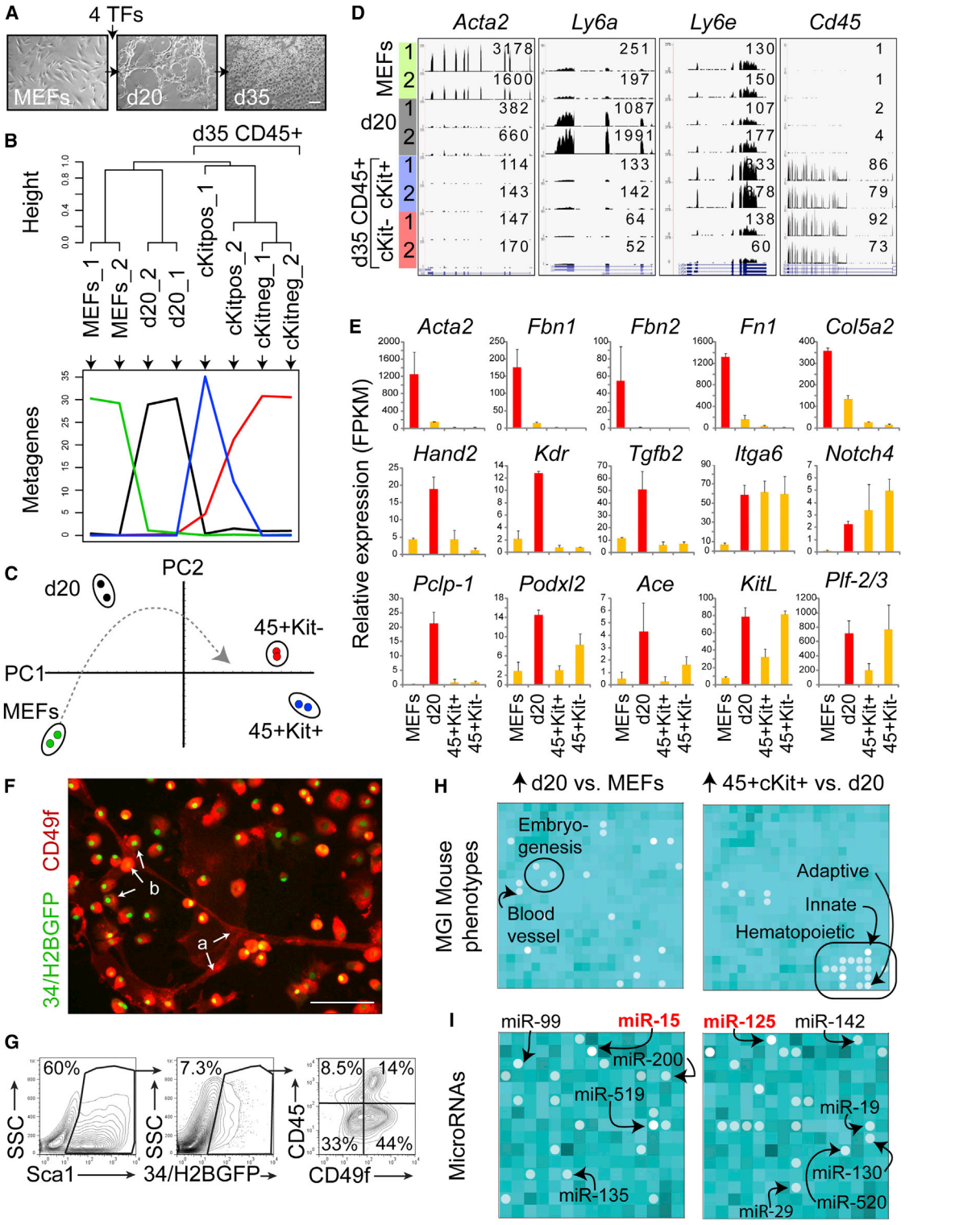

Figure 5. An Endothelial-like Gene-Expression Program Precedes Hematopoietic Specification

MEFs were transduced with four TFs and plated on gelatin without cytokines. Global gene-expression levels in nontransduced MEFs, day 20 GFP$^+$Sca1$^+$Prom1$^+$, and day 35 GFP$^+$CD45$^+$cKit$^+$ and GFP$^+$CD45$^+$cKit$^-$ were profiled by mRNA-seq (biological replicates: 1 and 2).

(A) Pictures show morphology of profiled populations. The scale bar represents 100 μm.

(B) Ordered tree linkage displays clustering of the profiled samples and the metagenes that represent most of the variability associated with each cell transition.

(C) PCA shows the relative distances between samples and a hypothetical temporal trajectory.

(D) Reads were aligned to the mouse genome, and those that mapped to the *Acta2*, *Ly6a*, *Ly6e*, and *Cd45* genes are displayed as maximum read heights.

(legend continued on next page)

(FACS) and culturing for 10 days without Dox showed that these cells continue to express CD45 without continued expression of the exogenous TFs (Figure S6C). To address a possible requirement for further maturation, we developed a placental reaggregate culture system similar to one previously reported for VE-Cadherin$^+$CD45$^+$ cells and AGM (Taoudi et al., 2008). We reasoned that cellular and/or molecular elements in this tissue could facilitate the maturation of our programmed cells to a clonogenic "state." After 25 days of programming culture in the presence of Dox, induced cells were dissociated and reaggregated with irradiated mouse placental cells (E12.5). After 4 or 5 days of culture without Dox, reaggregates were dissociated and the cells were plated into semisolid media for colony-forming unit (cfu) assays (Figure 7B). We observed the emergence of hematopoietic (CD45$^+$) colonies under these conditions (Figures 7C, 7D, and S6D). Four-day reaggregate cultures generated more cfu than 5 day cultures (Figure 7C). As expected, no colonies were observed in aggregates containing only irradiated placental cells (n = 6). Colonies derived from cfu contain cells with diverse myeloid morphologies as well as blast-like cells (Figure 7E). As expected, the cells contain transgene integrations (M2rtTA and Gata2) (Figure 7F). These data further support the specification of definitive hematopoietic cells by the four transcription factors.

DISCUSSION

We show that the combination of Gata2, Gfi1b, cFos, and Etv6 efficiently activates the 34/H2BGFP reporter and induces hematopoietic colonies from MEFs. Although Gata2, Gfi1b, and cFos are sufficient, Etv6 increases the efficiency up to 6%. Transduced MEFs first organize into circular endothelial-like structures that proceed to generate hematopoietic cells with specifying HSC gene-expression and cell-surface phenotypes. After placental reaggregation culture, induced cells acquire in vitro cfu activity. Thus, we provide strong evidence that a complex definitive hemogenic program can be recapitulated in vitro with a small number of TFs.

Genetic experiments show that the zinc-finger TF Gata2 is essential for all hematopoietic lineages (Tsai et al., 1994). Mutant *Gata2*$^{-/-}$ mice die at E11.5 and show placental neovascularization defects caused by reduced secretion of angiogenic proliferins (Ma et al., 1997; Tsai et al., 1994). Gfi1b is a SNAG (Snail-Gfi) domain transcriptional repressor. *Gfi1b*$^{-/-}$ mutants die at E15 from defects in definitive erythroid and megakaryocytic lineages but have normal vasculature (Lancrin et al., 2012; Saleque et al., 2002). A recent study identified a positive correlation between *Gata2* and *Gfi1b* expression at the level of single HSCs (Moignard et al., 2013). Gata2, Gfi1b, and cFos are essential for 34/H2BGFP reporter activation and induction of hemogenic colonies. The cFos TF is a component of the AP-1 complex via dimerization with cJun proteins. Mice lacking cFos have bone, hematopoietic, and placental defects (Johnson et al., 1992; Wang et al., 1992). In endothelial cells, AP-1 cooperates with Gata2 to induce key endothelial and inflammatory genes (Linnemann et al., 2011). Indeed, cFos promotes angiogenesis (Marconcini et al., 1999), and Fra-1, a related TF, is required for placental angiogenesis (Schreiber et al., 2000). A low level of HSC activity in *cFos*$^{-/-}$ placentas has been suggested (Ottersbach and Dzierzak, 2005), and *cFos* and *FosB* are specifically enriched in specifying HSCs (McKinney-Freeman et al., 2012). In our system, cFos may act by directly promoting endothelial and hematopoietic gene expression, but the possibility of a cell-proliferation function analogous to cMyc in iPSC reprogramming cannot be ruled out. The Ets-family TF Etv6 is not essential but increases reporter-activation efficiency. It is possible that the increased efficiency is due to enhanced cell survival. Mutant *Etv6*$^{-/-}$ mice have defects in yolk-sac angiogenesis and HSC survival (Hock et al., 2004b; Wang et al., 1997). It is perhaps surprising that exogenous Runx1 is not required for triggering the hemogenic process; however, Gata2, cFos, and Ets bind to *Runx1* regulatory elements and activate expression (Linnemann et al., 2011; Nottingham et al., 2007; Wilson et al., 2010). Indeed, at day 40, endogenous *Runx1* was upregulated in GFP$^+$CD45$^+$ cells. Taken together, these data highlight the balance between endothelial and hematopoietic traits during the generation of hematopoietic cells.

Induction of CD45$^+$ hematopoietic cells occurs 30–40 days after TF transduction. Emergent CD45$^+$cKit$^+$ cells have a gene-expression profile characteristic of bona fide HSCs. We show activation of the Notch and Cxcr4 pathways, both with functions in definitive hematopoiesis. Predicted targets of several miRNAs, including miR-125, are expressed in CD45$^+$cKit$^+$ cells. We also demonstrate a subpopulation with a LT-HSC phenotype; CD150$^+$CD48$^-$cKit$^+$ cells are present within emerging CD45$^+$ Sca1$^+$ cells. In addition, 34/H2BGFP expression is highest in CD45$^+$Sca1$^+$ cells. Emergent CD45$^+$ cells have an overall transcription profile highly similar to nascent or specifying HSCs from the AGM and placenta and express fetal HSC markers such as *Cd93/AA4.1*. These data further highlight the specification of hemogenesis by Gata2, cFos, Gfi1b, and Etv6. Culture conditions have an impact on reprogramming. Differential cytokine (IL-3 and IL-6) and substrate (AFT024 and gelatin) effects at different stages underscore the stepwise nature of this process. Reaggregate culture with placental cells at the liquid-gas interface promotes the maturation of specified cells into clonogenic

(E) The expression levels of fibroblast-specific genes in MEFs (red bars, upper panel) and genes overrepresented at day 20 (red bars, lower two panels) are shown as FPKM mean values ± SEM.
(F) MEFs were transduced with four TFs and analyzed at day 35 by immunofluorescence for GFP (green) and CD49f staining (red). (a) CD49f$^+$ endothelial-like and (b) small semiadherent GFP$^+$CD49f$^+$ cells are highlighted. The scale bar represents 100 μm.
(G) Flow plots show the expression of CD49f in the CD45$^+$ and CD45$^-$ population.
(H) Statistically significant genes upregulated from day 0 MEFs to day 20 and from day 20 to day 35 CD45$^+$cKit$^+$ cells were analyzed for gene-list enrichment with gene-set libraries created from level 4 of the MGI mouse phenotype ontology using Network2Canvas (http://maayanlab.net/N2C/). Phenotype categories are organized on the grid according to gene-list similarity; enriched categories are highlighted by circles. Circle brightness represents increasingly significant p values. Relevant terms are highlighted.
(I) Analysis using a gene-set library created from the miRNA prediction tool TargetScan. MiRNAs implicated in endothelial cells (left panel) or HSPCs (right panel) are highlighted. See also Figures S4 and S5.

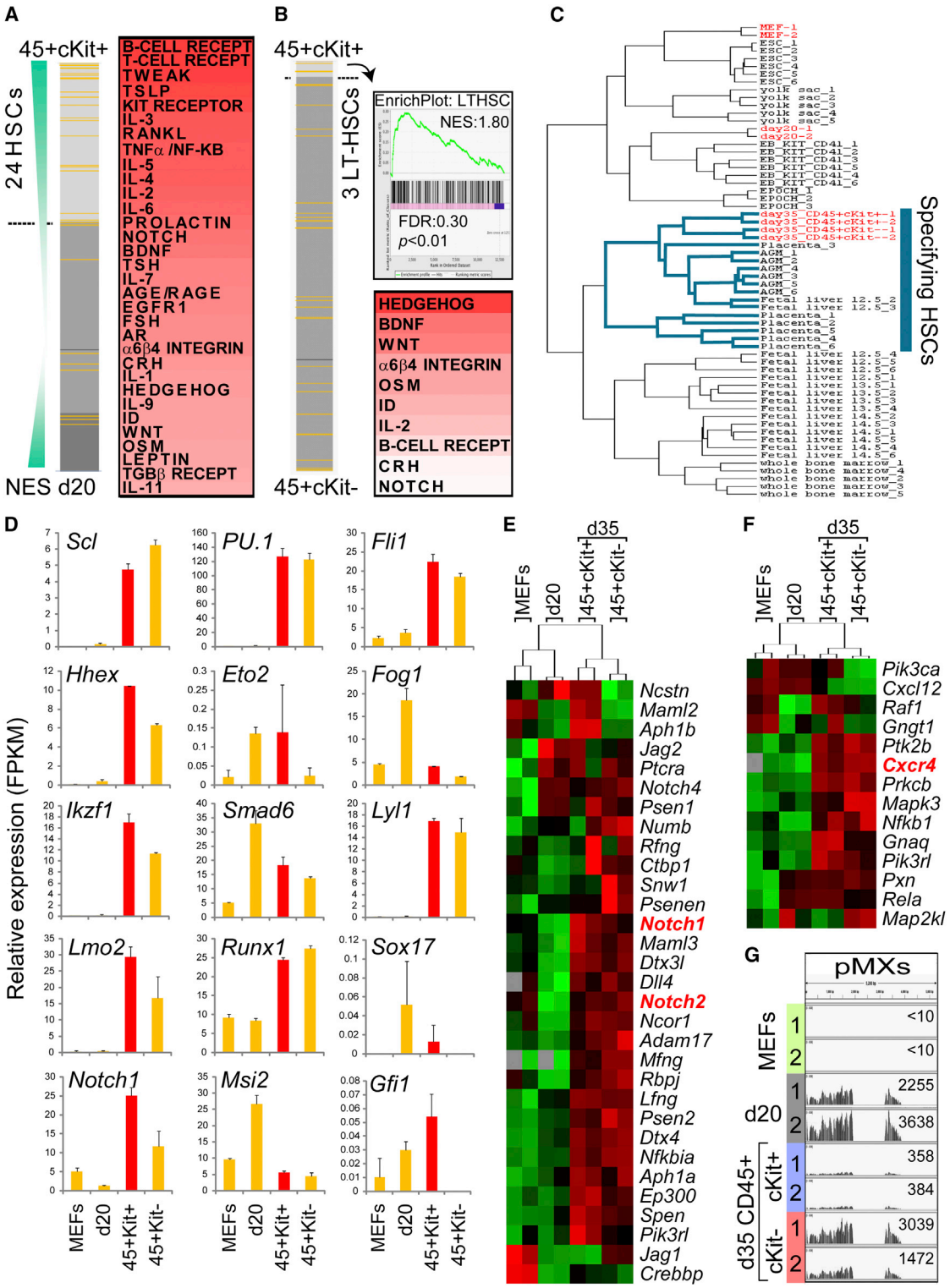

Figure 6. Specified Hematopoietic Cells Display Hallmarks of Definitive Hematopoiesis

(A) GSEA for day 20 and day 35 GFP$^+$CD45$^+$cKit$^+$ samples. Gene-expression lists were analyzed for enrichment of gene sets present in the Molecular Signatures Database (MSigDB; 1,888 gene sets, gene size 0–5,000). Orange lines represent HSC data sets and gray lines represent non-HSC data sets ordered according to the normalized enrichment score (NES). The dashed line highlights the cutoff FDR (FDR = 0.25). Right panels show GSEA of NetPath-annotated signaling pathways. Only enriched pathways are shown (FDR < 0.25, colored according to NES).

(B) GSEA for day 35 CD45$^+$cKit$^+$ and CD45$^+$cKit$^-$ cells. The dashed line highlights the cutoff (FDR = 0.35). The right panel shows the enrichment plot for one LT-HSC gene set.

(legend continued on next page)

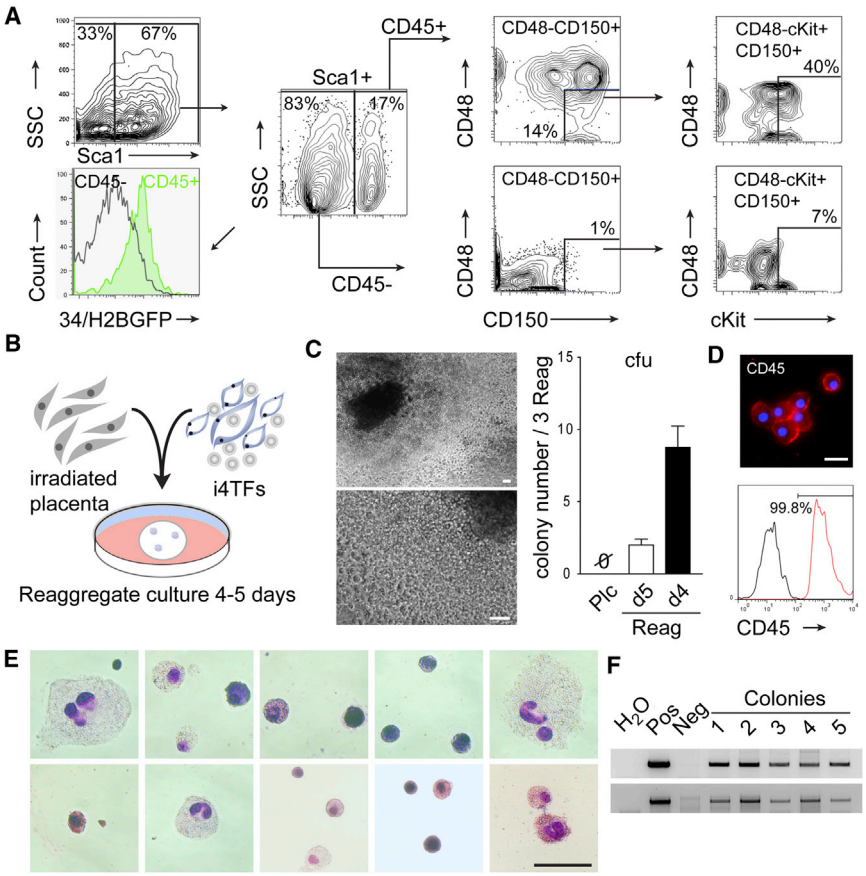

Figure 7. Specified Cells Contain a Subpopulation with a LT-HSC Cell-Surface Phenotype and Generate In Vitro Colonies after Reaggregation Culture

(A) A subpopulation of CD150$^+$CD48$^-$cKit$^+$ is present in the Sca1$^+$CD45$^+$ population 30 days after transduction. The histogram shows reporter expression in the CD45$^+$ and CD45$^-$ compartments of the Sca1$^+$ population. The Sca1$^+$CD45$^+$CD150$^+$CD48$^-$ and Sca1$^+$CD45$^+$CD150$^+$CD48$^-$cKit$^+$ populations represent 1.6% and 0.64% of total cells, respectively.

(B) Reaggregation strategy for cells generated with four inducible TFs (i4TFs) at day 25 (+Dox) and irradiated mouse placental tissue (E12.5). Reaggregates were cultured (−Dox) for 4 or 5 days before transfer to methylcellulose-containing media.

(C) Clonogenic activity in semisolid media after a reaggregation step of 4 (d4) or 5 (d5) days. Control irradiated placenta alone (Plc) did not generate colonies (n = 6). Colony numbers per three plated reaggregates (Reag) are shown (mean ± SEM). Scale bars represent 100 μm.

(D) One colony was manually picked and analyzed via immunofluorescence for CD45 (red). DAPI staining is shown in blue. The flow-cytometry plot shows the percentage of CD45-positive cells (red line) in three pooled colonies. The control staining is shown in black. The scale bar represents 20 μm.

(E) Mixed cell morphologies are observed from cells within the colonies, shown by modified Giemsa staining. The scale bar represents 100 μm.

(F) Integration of inducible lentivirus in five independent colonies was confirmed by PCR. The forward primer is in the lentiviral vector (tetO), and the reverse is in the coding sequence of *Gata2* (lower panel) or *M2rtTA* (upper panel).

See also Figure S6.

progenitors, highlighting the role of a permissive environment for progenitor cell maturation. It will be of critical importance to develop more-defined culture methods for the controlled maturation of in vitro-programmed as well as embryo-derived nascent HSCs into definitive, fully functional HSCs.

We show that hematopoietic cells originate from endothelial-like precursor cells that express Sca1 (mainly from the *Ly6a* locus) and Prom1. *Ly6a* is expressed before HSC emergence, and *Gata2* haploinsufficient embryos have a 10-fold decrease in *Ly6a*-GFP$^+$ aortic endothelial cells (Ling et al., 2004), demonstrating a link between *Gata2* and *Ly6a* in the AGM. The role of Prom1 is obscure in the mouse; however, in humans it marks endothelial progenitor cells (Masuda et al., 2011). Indeed, it has been shown that a human umbilical cord CD34$^+$Prom1$^+$ population gives rise to both endothelial and hematopoietic cells (Wu et al., 2007). *Prom1* is a target of Gata2 and AP-1 in these two lineages (Linnemann et al., 2011; Wilson et al., 2010). At day 20, we detect expression of numerous additional endothelial genes (*Id1*, *Nos3*, *KitL*, and *Cd34*) at continually increasing levels. Other genes implicated in HSC emergence, including *Podxl*, *Ace*, *Kdr*, *Smad6*, and *Scl*, are also expressed at this time. At day 35, we detect Tie2, VE-Cadherin, and CD31 in association with hematopoietic cell emergence. There is great interest in defining HSC precursors in vivo, and our data may provide useful markers. Indeed, we demonstrate the expression of potential markers including integrin α-6 (*Itga6*) (CD49f), shown to be present on human LT-HSCs (Notta et al., 2011). It will be interesting in future studies to determine whether cells with the Sca1$^+$Prom1$^+$CD34$^+$CD49f$^+$ precursor phenotype are present in hemogenic sites during embryonic development. Proliferin and proliferin-related genes *Plf*, *Plf-2/3*, and *Plf-4* that have defined angiogenic functions are also activated (Ma et al.,

(C) Hierarchical clustering showing the integration of gene-expression data from programmed cells (highlighted in red) with HSCs at several developmental stages (data from McKinney-Freeman et al., 2012).

(D) The expression of TFs implicated in HSC specification and maintenance is shown as FPKM values and highlighted in CD45$^+$cKit$^+$ (red bars). Data are represented as mean ± SEM.

(E and F) Heatmap showing the enriched expression of the Notch (E) and Cxcr4 (F) pathway components in CD45$^+$ cells. Notch1, Notch2, and Cxcr4 receptors are highlighted in red. FPKM values were analyzed by Cluster and displayed by TreeView. Red designates increased expression and green designates decreased expression relative to the mean. Gray designates no detection.

(G) MEFs and day 20 and day 35 CD45$^+$cKit$^+$ and CD45$^+$cKit$^-$ replicates (1 and 2) were analyzed for expression of pMXs vector-derived sequences. Graphs show reads that align to the pMXs long terminal repeats, and the maximum read heights are displayed.

1997). Low expression of additional hematopoietic genes, for example *Csfr1*, is observed at day 20, suggesting that the endothelial-like cells may already be primed for hematopoietic competence as previously reported in the AGM (Minehata et al., 2002).

The induction of human progenitor cells has been reported (Szabo et al., 2010). However, overexpression of Oct4 is likely to induce plastic intermediates (perhaps on the way to pluripotency) that can be selected for hematopoietic lineages in appropriate culture conditions. Extending our directed programming studies to the human system may shed light on specification of HSPCs during human embryonic development, as well as robust in vitro methods to generate such cells.

Collectively, our results show that TFs are sufficient for efficient generation of hematopoietic cells from fibroblasts. This process is dynamic and proceeds through an endothelial-like intermediate. Emergent hematopoietic cells exhibit LT-HSC gene-expression and cell-surface phenotypes. Our results support the view that hematopoietic specification is a multistep process and underscore the requirement for endothelial-like intermediates. In summary, we demonstrate that a complex and progressive developmental process can be initiated and sustained in vitro with a simple combination of TFs and provide insights into the molecular mechanisms of HSPC specification. These studies also provide a platform for the future development of patient-specific HSPCs as well as other blood cells.

EXPERIMENTAL PROCEDURES

Mice, MEF Isolation, and Culture

Individual transgenic CD34-tTA (Dan Tenen, Harvard Medical School) and TetO-H2BGFP (The Jackson Laboratory) mouse lines were established in the C57BL/6 (CD45.2) background. Double-transgenic (designated 34/H2BGFP) MEFs were derived from crosses of the two transgenic mice. Cells from each E14.5 embryo were plated in MEF media, grown for 4–7 days until confluent, and then split once (Supplemental Experimental Procedures). MEFs were sorted to remove residual $CD45^+$ and GFP^+ cells that could represent cells with hematopoietic potential and cultured for two additional passages before plating for retroviral transduction. Animal experiments and procedures were approved by the Institutional Animal Care and Use Committee and conducted in accordance with the Animal Welfare Act.

Viral Transduction and Cell Culture

34/H2BGFP MEFs were seeded at a density of 25,000 cells per well on 0.1% gelatin-coated 6-well plates and incubated overnight with pools of TF pMXs retroviruses or pFUW lentiviruses in media supplemented with 8 μg/ml polybrene. Equal multiplicities of infection of individual viral particles were applied. Transductions with mCherry in pMXs or mOrange in pFUW resulted in >95% efficiency. After 16–20 hr, media was replaced with fresh MEF media supplemented with Dox (1 μg/ml) in the case of inducible vectors. At day 4 posttransduction, cells were dissociated with TrypLE Express, and 10,000 cells per well were plated on 0.1% gelatin-coated 6-well plates containing mitotically inactivated AFT024 stroma. All cultures were maintained in MyeloCult media (M5300; Stem Cell Technologies) supplemented with hydrocortisone (10^{-6} M; Stem Cell Technologies) with or without 100 ng/ml SCF, 100 ng/ml Flt3L, 20 ng/ml IL-3, and 20 ng/ml IL-6 (R&D Systems), with the exception of methylcellulose cultures, for which cytokine complete MethoCult media was used (M3434; Stem Cell Technologies) supplemented with 10 ng/ml TPO (R&D Systems). Media were changed every 6 days for the duration of the cultures. Emerging GFP^+ colonies were counted 21–25 days posttransduction. Experimental details for immunofluorescence, FACS, quantitative RT-PCR (qRT-PCR), and reaggregation cultures are provided in Supplemental Experimental Procedures.

mRNA-Seq Library Preparation, Sequencing, and Analysis

FACS-isolated cells were lysed in Trizol (Ambion). RNA integrity was evaluated using a eukaryotic RNA 6000 Nano chip on an Agilent 2100 Bioanalyzer (Agilent Technologies). Up to 1 μg of total RNA from each sample was used for library preparation with the TruSeq RNA Sample Preparation Kit (Illumina). A common adaptor was used for all samples, and barcode sequences present in the reverse primer were introduced by 12–16 cycles of amplification (Table S4). Each library was assessed for quality and size distribution using an Agilent DNA High Sensitivity Assay Bioanalyzer chip and quantified by real-time PCR. Equimolar amounts of each barcoded library were mixed and single-end sequenced on an Illumina HiSeq Sequencing System. For each sample, 14–21.7 M 50-nt reads were obtained, preprocessed with the FASTX-Toolkit suite (http://hannonlab.cshl.edu/fastx_toolkit/), and aligned to the mouse genome (*Mus musculus* mm9 assembly) using TopHat mapper. Additional analytical details are provided in Supplemental Experimental Procedures.

ACCESSION NUMBERS

mRNA-seq data were deposited in the Gene Expression Omnibus database under accession number GSE47497.

SUPPLEMENTAL INFORMATION

Supplemental Information includes Supplemental Experimental Procedures, six figures, six tables, and two movies and can be found with this article online at http://dx.doi.org/10.1016/j.stem.2013.05.024.

ACKNOWLEDGMENTS

We thank D. Tenen (Harvard Medical School) for the huCD34tTa transgenic mouse. We thank D.F. Lee, Y.S. Ang, S. Mulero-Navarro, A. Freire, and the members of the Lemischka/Moore laboratory for useful discussions and Y. Liu for laboratory management. We would like to thank M. Rendl and V. Gouon-Evans and their laboratories for their assistance. We thank T. Schroeder and K. Kokkaliaris for advice with live imaging and F. González for inducible vectors. We thank M. Baron and S. Ghaffari for critical reading of the manuscript. We would also like to thank the Mount Sinai hESC/hiPSC Shared Resource Facility and S. D'Souza for help with materials and protocols and the Mount Sinai Genomics, Flow Cytometry, and Mouse facilities. C.F.P. is a recipient of an EMBO Long-term Postdoctoral Fellowship. J.C.K. and A.N.K are supported by the NIH grants 5K08HL111330 and 5T32HL007824-15; A.M. by R01GM098316 and R01DK088541.

Received: October 9, 2012
Revised: May 16, 2013
Accepted: May 29, 2013
Published: June 13, 2013

REFERENCES

Bertrand, J.Y., Chi, N.C., Santoso, B., Teng, S., Stainier, D.Y., and Traver, D. (2010). Haematopoietic stem cells derive directly from aortic endothelium during development. Nature *464*, 108–111.

Boisset, J.C., van Cappellen, W., Andrieu-Soler, C., Galjart, N., Dzierzak, E., and Robin, C. (2010). In vivo imaging of haematopoietic cells emerging from the mouse aortic endothelium. Nature *464*, 116–120.

Burda, P., Laslo, P., and Stopka, T. (2010). The role of PU.1 and GATA-1 transcription factors during normal and leukemogenic hematopoiesis. Leukemia *24*, 1249–1257.

Chen, M.J., Li, Y., De Obaldia, M.E., Yang, Q., Yzaguirre, A.D., Yamada-Inagawa, T., Vink, C.S., Bhandoola, A., Dzierzak, E., and Speck, N.A. (2011). Erythroid/myeloid progenitors and hematopoietic stem cells originate from distinct populations of endothelial cells. Cell Stem Cell *9*, 541–552.

Deneault, E., Cellot, S., Faubert, A., Laverdure, J.P., Fréchette, M., Chagraoui, J., Mayotte, N., Sauvageau, M., Ting, S.B., and Sauvageau, G. (2009). A functional screen to identify novel effectors of hematopoietic stem cell activity. Cell *137*, 369–379.

Eilken, H.M., Nishikawa, S., and Schroeder, T. (2009). Continuous single-cell imaging of blood generation from haemogenic endothelium. Nature *457*, 896–900.

Feng, R., Desbordes, S.C., Xie, H., Tillo, E.S., Pixley, F., Stanley, E.R., and Graf, T. (2008). PU.1 and C/EBPalpha/beta convert fibroblasts into macrophage-like cells. Proc. Natl. Acad. Sci. USA *105*, 6057–6062.

Guo, S., Lu, J., Schlanger, R., Zhang, H., Wang, J.Y., Fox, M.C., Purton, L.E., Fleming, H.H., Cobb, B., Merkenschlager, M., et al. (2010). MicroRNA miR-125a controls hematopoietic stem cell number. Proc. Natl. Acad. Sci. USA *107*, 14229–14234.

Hara, T., Nakano, Y., Tanaka, M., Tamura, K., Sekiguchi, T., Minehata, K., Copeland, N.G., Jenkins, N.A., Okabe, M., Kogo, H., et al. (1999). Identification of podocalyxin-like protein 1 as a novel cell surface marker for hemangioblasts in the murine aorta-gonad-mesonephros region. Immunity *11*, 567–578.

Hock, H., Hamblen, M.J., Rooke, H.M., Schindler, J.W., Saleque, S., Fujiwara, Y., and Orkin, S.H. (2004a). Gfi-1 restricts proliferation and preserves functional integrity of haematopoietic stem cells. Nature *431*, 1002–1007.

Hock, H., Meade, E., Medeiros, S., Schindler, J.W., Valk, P.J., Fujiwara, Y., and Orkin, S.H. (2004b). Tel/Etv6 is an essential and selective regulator of adult hematopoietic stem cell survival. Genes Dev. *18*, 2336–2341.

Johnson, R.S., Spiegelman, B.M., and Papaioannou, V. (1992). Pleiotropic effects of a null mutation in the c-fos proto-oncogene. Cell *71*, 577–586.

Kim, I., Saunders, T.L., and Morrison, S.J. (2007). Sox17 dependence distinguishes the transcriptional regulation of fetal from adult hematopoietic stem cells. Cell *130*, 470–483.

Kissa, K., and Herbomel, P. (2010). Blood stem cells emerge from aortic endothelium by a novel type of cell transition. Nature *464*, 112–115.

Klug, C.A., Cheshier, S., and Weissman, I.L. (2000). Inactivation of a GFP retrovirus occurs at multiple levels in long-term repopulating stem cells and their differentiated progeny. Blood *96*, 894–901.

Kumano, K., Chiba, S., Kunisato, A., Sata, M., Saito, T., Nakagami-Yamaguchi, E., Yamaguchi, T., Masuda, S., Shimizu, K., Takahashi, T., et al. (2003). Notch1 but not Notch2 is essential for generating hematopoietic stem cells from endothelial cells. Immunity *18*, 699–711.

Lancrin, C., Sroczynska, P., Stephenson, C., Allen, T., Kouskoff, V., and Lacaud, G. (2009). The haemangioblast generates haematopoietic cells through a haemogenic endothelium stage. Nature *457*, 892–895.

Lancrin, C., Mazan, M., Stefanska, M., Patel, R., Lichtinger, M., Costa, G., Vargel, O., Wilson, N.K., Möröy, T., Bonifer, C., et al. (2012). GFI1 and GFI1B control the loss of endothelial identity of hemogenic endothelium during hematopoietic commitment. Blood *120*, 314–322.

Li, Z., Chen, M.J., Stacy, T., and Speck, N.A. (2006). Runx1 function in hematopoiesis is required in cells that express Tek. Blood *107*, 106–110.

Ling, K.W., Ottersbach, K., van Hamburg, J.P., Oziemlak, A., Tsai, F.Y., Orkin, S.H., Ploemacher, R., Hendriks, R.W., and Dzierzak, E. (2004). GATA-2 plays two functionally distinct roles during the ontogeny of hematopoietic stem cells. J. Exp. Med. *200*, 871–882.

Linnemann, A.K., O'Geen, H., Keles, S., Farnham, P.J., and Bresnick, E.H. (2011). Genetic framework for GATA factor function in vascular biology. Proc. Natl. Acad. Sci. USA *108*, 13641–13646.

Lujan, E., Chanda, S., Ahlenius, H., Südhof, T.C., and Wernig, M. (2012). Direct conversion of mouse fibroblasts to self-renewing, tripotent neural precursor cells. Proc. Natl. Acad. Sci. USA *109*, 2527–2532.

Ma, G.T., Roth, M.E., Groskopf, J.C., Tsai, F.Y., Orkin, S.H., Grosveld, F., Engel, J.D., and Linzer, D.I. (1997). GATA-2 and GATA-3 regulate trophoblast-specific gene expression in vivo. Development *124*, 907–914.

Marconcini, L., Marchio, S., Morbidelli, L., Cartocci, E., Albini, A., Ziche, M., Bussolino, F., and Oliviero, S. (1999). c-fos-induced growth factor/vascular endothelial growth factor D induces angiogenesis in vivo and in vitro. Proc. Natl. Acad. Sci. USA *96*, 9671–9676.

Masuda, H., Alev, C., Akimaru, H., Ito, R., Shizuno, T., Kobori, M., Horii, M., Ishihara, T., Isobe, K., Isozaki, M., et al. (2011). Methodological development of a clonogenic assay to determine endothelial progenitor cell potential. Circ. Res. *109*, 20–37.

McKinney-Freeman, S., Cahan, P., Li, H., Lacadie, S.A., Huang, H.T., Curran, M., Loewer, S., Naveiras, O., Kathrein, K.L., Konantz, M., et al. (2012). The transcriptional landscape of hematopoietic stem cell ontogeny. Cell Stem Cell *11*, 701–714.

Medvinsky, A., Rybtsov, S., and Taoudi, S. (2011). Embryonic origin of the adult hematopoietic system: advances and questions. Development *138*, 1017–1031.

Minehata, K., Mukouyama, Y.S., Sekiguchi, T., Hara, T., and Miyajima, A. (2002). Macrophage colony stimulating factor modulates the development of hematopoiesis by stimulating the differentiation of endothelial cells in the AGM region. Blood *99*, 2360–2368.

Moepps, B., Braun, M., Knöpfle, K., Dillinger, K., Knöchel, W., and Gierschik, P. (2000). Characterization of a Xenopus laevis CXC chemokine receptor 4: implications for hematopoietic cell development in the vertebrate embryo. Eur. J. Immunol. *30*, 2924–2934.

Moignard, V., Macaulay, I.C., Swiers, G., Buettner, F., Schütte, J., Calero-Nieto, F.J., Kinston, S., Joshi, A., Hannah, R., Theis, F.J., et al. (2013). Characterization of transcriptional networks in blood stem and progenitor cells using high-throughput single-cell gene expression analysis. Nat. Cell Biol. *15*, 363–372.

Moore, K.A., Ema, H., and Lemischka, I.R. (1997). In vitro maintenance of highly purified, transplantable hematopoietic stem cells. Blood *89*, 4337–4347.

North, T., Gu, T.L., Stacy, T., Wang, Q., Howard, L., Binder, M., Marín-Padilla, M., and Speck, N.A. (1999). Cbfa2 is required for the formation of intra-aortic hematopoietic clusters. Development *126*, 2563–2575.

Notta, F., Doulatov, S., Laurenti, E., Poeppl, A., Jurisica, I., and Dick, J.E. (2011). Isolation of single human hematopoietic stem cells capable of long-term multilineage engraftment. Science *333*, 218–221.

Nottingham, W.T., Jarratt, A., Burgess, M., Speck, C.L., Cheng, J.F., Prabhakar, S., Rubin, E.M., Li, P.S., Sloane-Stanley, J., Kong-A-San, J., and de Bruijn, M.F. (2007). Runx1-mediated hematopoietic stem-cell emergence is controlled by a Gata/Ets/SCL-regulated enhancer. Blood *110*, 4188–4197.

Ottersbach, K., and Dzierzak, E. (2005). The murine placenta contains hematopoietic stem cells within the vascular labyrinth region. Dev. Cell *8*, 377–387.

Pereira, C.F., Lemischka, I.R., and Moore, K. (2012). Reprogramming cell fates: insights from combinatorial approaches. Ann. N Y Acad. Sci. *1266*, 7–17.

Porcher, C., Swat, W., Rockwell, K., Fujiwara, Y., Alt, F.W., and Orkin, S.H. (1996). The T cell leukemia oncoprotein SCL/tal-1 is essential for development of all hematopoietic lineages. Cell *86*, 47–57.

Radomska, H.S., Gonzalez, D.A., Okuno, Y., Iwasaki, H., Nagy, A., Akashi, K., Tenen, D.G., and Huettner, C.S. (2002). Transgenic targeting with regulatory elements of the human CD34 gene. Blood *100*, 4410–4419.

Ring, K.L., Tong, L.M., Balestra, M.E., Javier, R., Andrews-Zwilling, Y., Li, G., Walker, D., Zhang, W.R., Kreitzer, A.C., and Huang, Y. (2012). Direct reprogramming of mouse and human fibroblasts into multipotent neural stem cells with a single factor. Cell Stem Cell *11*, 100–109.

Rodrigues, N.P., Janzen, V., Forkert, R., Dombkowski, D.M., Boyd, A.S., Orkin, S.H., Enver, T., Vyas, P., and Scadden, D.T. (2005). Haploinsufficiency of GATA-2 perturbs adult hematopoietic stem-cell homeostasis. Blood *106*, 477–484.

Saleque, S., Cameron, S., and Orkin, S.H. (2002). The zinc-finger proto-oncogene Gfi-1b is essential for development of the erythroid and megakaryocytic lineages. Genes Dev. *16*, 301–306.

Schaniel, C., and Moore, K.A. (2009). Genetic models to study quiescent stem cells and their niches. Ann. N Y Acad. Sci. *1176*, 26–35.

Schreiber, M., Wang, Z.Q., Jochum, W., Fetka, I., Elliott, C., and Wagner, E.F. (2000). Placental vascularisation requires the AP-1 component fra1. Development *127*, 4937–4948.

Sinka, L., Biasch, K., Khazaal, I., Péault, B., and Tavian, M. (2012). Angiotensin-converting enzyme (CD143) specifies emerging lympho-hematopoietic progenitors in the human embryo. Blood *119*, 3712–3723.

Souroullas, G.P., Salmon, J.M., Sablitzky, F., Curtis, D.J., and Goodell, M.A. (2009). Adult hematopoietic stem and progenitor cells require either Lyl1 or Scl for survival. Cell Stem Cell *4*, 180–186.

Szabo, E., Rampalli, S., Risueño, R.M., Schnerch, A., Mitchell, R., Fiebig-Comyn, A., Levadoux-Martin, M., and Bhatia, M. (2010). Direct conversion of human fibroblasts to multilineage blood progenitors. Nature *468*, 521–526.

Takahashi, K., and Yamanaka, S. (2006). Induction of pluripotent stem cells from mouse embryonic and adult fibroblast cultures by defined factors. Cell *126*, 663–676.

Taoudi, S., Gonneau, C., Moore, K., Sheridan, J.M., Blackburn, C.C., Taylor, E., and Medvinsky, A. (2008). Extensive hematopoietic stem cell generation in the AGM region via maturation of VE-cadherin+CD45+ pre-definitive HSCs. Cell Stem Cell *3*, 99–108.

Tsai, F.Y., Keller, G., Kuo, F.C., Weiss, M., Chen, J., Rosenblatt, M., Alt, F.W., and Orkin, S.H. (1994). An early haematopoietic defect in mice lacking the transcription factor GATA-2. Nature *371*, 221–226.

Wang, Z.Q., Ovitt, C., Grigoriadis, A.E., Möhle-Steinlein, U., Rüther, U., and Wagner, E.F. (1992). Bone and haematopoietic defects in mice lacking c-fos. Nature *360*, 741–745.

Wang, L.C., Kuo, F., Fujiwara, Y., Gilliland, D.G., Golub, T.R., and Orkin, S.H. (1997). Yolk sac angiogenic defect and intra-embryonic apoptosis in mice lacking the Ets-related factor TEL. EMBO J. *16*, 4374–4383.

Wilson, N.K., Foster, S.D., Wang, X., Knezevic, K., Schütte, J., Kaimakis, P., Chilarska, P.M., Kinston, S., Ouwehand, W.H., Dzierzak, E., et al. (2010). Combinatorial transcriptional control in blood stem/progenitor cells: genome-wide analysis of ten major transcriptional regulators. Cell Stem Cell *7*, 532–544.

Wu, X., Lensch, M.W., Wylie-Sears, J., Daley, G.Q., and Bischoff, J. (2007). Hemogenic endothelial progenitor cells isolated from human umbilical cord blood. Stem Cells *25*, 2770–2776.

Yin, K.J., Olsen, K., Hamblin, M., Zhang, J., Schwendeman, S.P., and Chen, Y.E. (2012). Vascular endothelial cell-specific microRNA-15a inhibits angiogenesis in hindlimb ischemia. J. Biol. Chem. *287*, 27055–27064.

Zovein, A.C., Hofmann, J.J., Lynch, M., French, W.J., Turlo, K.A., Yang, Y., Becker, M.S., Zanetta, L., Dejana, E., Gasson, J.C., et al. (2008). Fate tracing reveals the endothelial origin of hematopoietic stem cells. Cell Stem Cell *3*, 625–636.